Skeletal Radiol (2015) 44:1735–1743
DOI 10.1007/s00256-015-2224-3

SCIENTIFIC ARTICLE

The extensor carpi ulnaris pseudolesion: evaluation with microCT, histology, and MRI

Sayed Ali[1] · **Ryan Cunningham**[1] · **Mamta Amin**[2] · **Steven N. Popoff**[2] · **Feroze Mohamed**[1] · **Mary F. Barbe**[2]

Received: 16 January 2015 / Revised: 8 July 2015 / Accepted: 22 July 2015 / Published online: 6 August 2015

Abstract
Objective To determine if magic angle plays a role in apparent central increased signal intensity of the distal extensor carpi ulnaris tendon (ECU) on MRI, to see if histologic findings of tendon degeneration are associated with increased T1 or T2 tendon signal on MR imaging, and to determine the prevalence of the ECU "pseudolesion".
Materials and methods A standard 3 Tesla protocol was utilized to scan ten cadaveric wrists. A 40 mm length of 10 ECU and four extensor carpi radialis brevis (ECRB) tendons were immersion fixed before microCT scanning. Staining with Alcian blue, Masson's trichrome and Safranin O was performed before light microscopy. Fifty clinical wrist MRIs were also reviewed for the presence of increased T1 and/or T2 signal.
Results Central increased T1 and/or T2 signal was observed in 9 of 10 cadaveric ECU tendons, but not in ECRB tendons. MicroCT and histology showed inter-tendinous matrix between the two distal heads of the ECU. Increased mucoid degeneration correlated with increased MRI signal intensity. The tendon fibers were at a maximum of 8.39° to the longitudinal axis on microCT. Clinical MRIs showed increased T1 signal in 6 %, increased T2 signal in 8 %, increased T1 and T2 signal in 80 %, and 6 % showing no increased signal.
Conclusion Central increased T1 and/or T2 signal in the ECU tendon indicates the presence of normal inter-tendinous ground substance, with increased proteoglycan content (mucoid degeneration) responsible for increased signal intensity. None of the fibers were shown on microCT to approach the magic angle.

Keywords Tendon · Magic angle · Ground substance · Mucoid

✉ Sayed Ali
alisayan@tuhs.temple.edu

[1] Department of Radiology, Temple University Hospital, 3401 North Broad Street, Philadelphia, PA 19140, USA

[2] Department of Anatomy, Temple University School of Medicine, 3500 North Broad Street, Philadelphia, PA 19140, USA

Introduction

Ulnar-sided wrist pain is a common entity, and multiple etiologies are possible including triangular fibrocartilage injuries, osseous pathology including ulna styloid, pisiform, hamate fractures or contusion, carpal and distal radio-ulnar joint instability, ulnar impingement and impaction syndromes, ulnar nerve compression in Guyon's canal, and tendon-related pathology including tendinosis, tenosynovitis and tendon subluxation [1–3]. The extensor carpi ulnaris "pseudolesion" is a commonly seen entity that manifests as increased T1 and/or T2 signal within the central substance of the extensor carpi ulnaris (ECU) tendon at the level of the ulna styloid process, and is frequently interpreted as ECU tendinosis and, therefore, a potential cause for ulnar-sided pain. The ECU pseudolesion is characterized by central increased signal on axial T1- and T2-weighted images, with a normal tendon size and no associated fluid distention of the tendon sheath. Conversely, tendinosis is typically characterized by diffuse (not central) increased signal, with tendon enlargement and may be associated with tenosynovitis. This increased signal is seen only on the axial images (Figs. 1 and 2). A previously proposed explanation of the pseudolesion is spiraling or decussation of the two heads of the distal ECU, resulting in increased signal

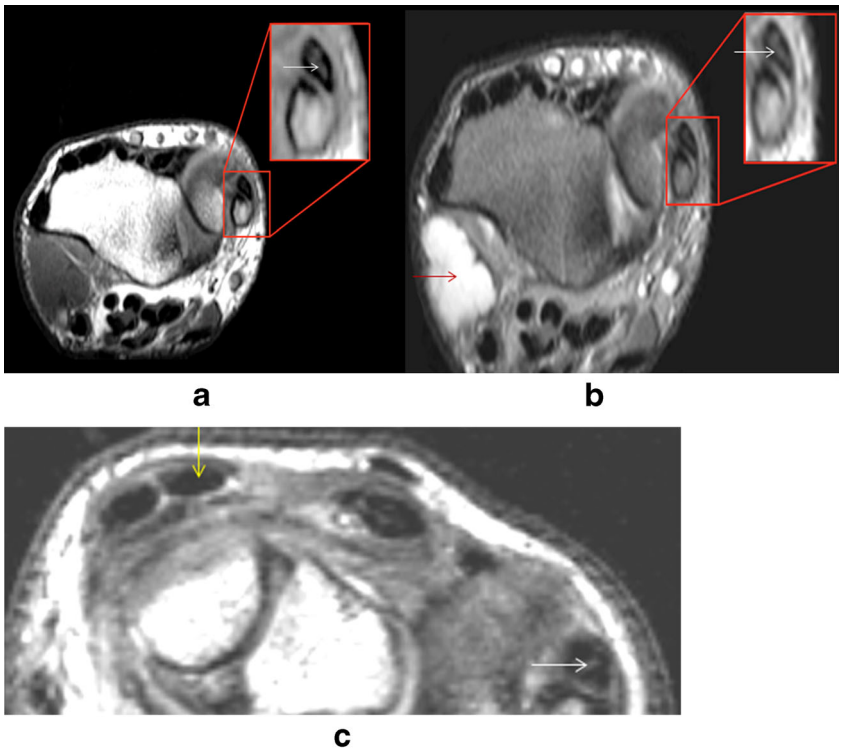

Fig. 1 42-year-old male. The ECU pseudolesion is observed as increased T1 (**a**) and T2 (**b**) signal (*white arrows*) centrally in the ECU tendon at the level of the ulna styloid process. Note incidental ganglion cyst (*red arrow*). Axial T1-weighted image in another patient (**c**) shows the homogenously dark ECRB tendon (*yellow arrow*), and the central increased signal in the ECU (*white arrow*) at the same window. Scans were performed on a Siemens Verio 3.0 Tesla MRI

as the spiraling fibers approach the "magic angle" in the standard scanning position with the patient in the prone position and the arm above the head [4]. Kalson et al. demonstrated that the fibers of the ECU tendon do spiral, but do not approach the magic angle anywhere along the course of the tendon, as the maximum angle to B0 was 8° [5]. Also, the T2 signal would be expected to be normal as sequences with a longer TE results in loss of the increased signal, if magic angle effect was in fact the etiology.Our aim was to determine the prevalence of the ECU pseudolesion, determine whether the "magic angle" effect plays a role in its pathogenesis, and to provide a possible pathologic explanation for the imaging findings.

Materials and methods

This study was performed after obtaining institutional review board approval from our institution.

Clinical

A retrospective review of 147 clinical MRI cases of the wrist, obtained between 2005 and 2013, was performed. The electronic medical records were reviewed for the presence of wrist pain involving the ulnar side, a history of overuse, prior trauma or surgery. If radiographs were available, these were reviewed for osseous fragments, post-traumatic or post-surgical change in the region of the ulna styloid base or distal ulna. MRIs with findings of tenosynovitis, tendon enlargement or attenuation suggesting tendinosis or partial/complete ECU tear, and prior trauma or surgery in the ulnar region were also excluded. Tendinosis is defined by diffuse (not central) intra-tendinous high signal accompanied by tendon thickening, and tenosynovitis as a qualitative excess of synovial fluid in the tendon sheath. Conversely, the ECU pseudolesion is characterized by central (not diffuse) increased signal on axial T1- and T2-weighted images with a normal tendon size. The severity was subjectively classified into mild, moderate or severe categories with an increasing signal intensity resulting in a higher grade. No cases demonstrated asymptomatic ECU tendinosis, tear or tenosynovitis. Of these 147 scans, 97 scans were excluded based on the aforementioned exclusion criteria.

The 50 scans that met the criteria for inclusion in our study were performed on either a General Electric (GE) 1.5 Tesla Signa Excite or Siemens 3 Tesla Verio scanner, and the wrists were imaged in the axial, coronal and sagittal planes utilizing spin echo T1 and fat-suppressed fast spin echo T2-weighted images, as well as as coronal 3D gradient echo images. The wrists were scanned in the "superman" position with the patient prone and the arm extended above the head, or in the supine position with the hand on the side in the neutral position. A dedicated wrist coil was used in all cases. Since the ECU pseudolesion is seen in the axial plane only, the axial parameters alone will be outlined below.

The 1.5 Tesla protocol included T1-weighted images with a TE of 20–25 milliseconds (ms), TR of 600–800 ms, slice thickness of 4 mm with a 1 mm gap, matrix of 358×224, field

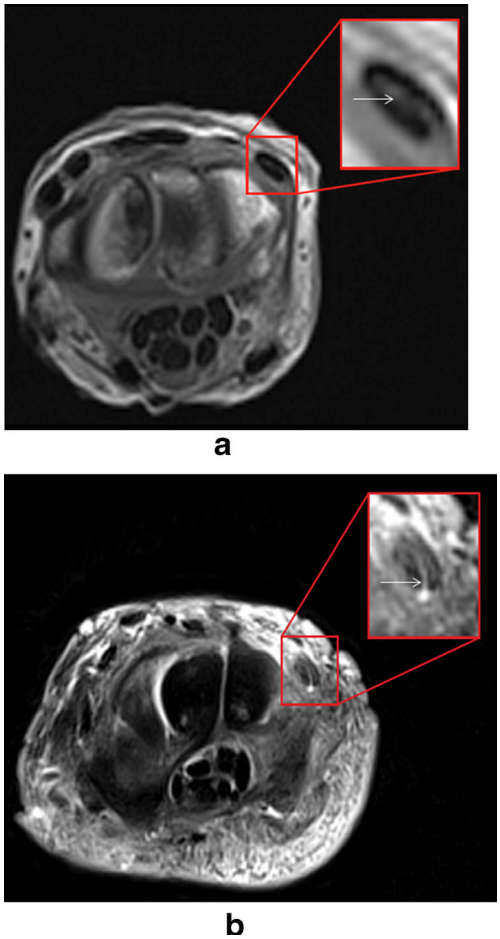

Fig. 2 71-year-old female cadaver. Axial T1 (**a**) and fat suppressed T2 (**b**) weighted images through cadaveric wrists demonstrating central increased signal on both sequences (*arrows in insets*) at the level of the ulna styloid process. This corresponds with increased signal observed at this location in MRI scans of clinical wrists. Scans were performed on a Siemens Verio 3.0 Tesla MRI

of view (FOV) of 120 mm and the number of excitations (NEX) was 1. The T2-weighted images utilized a TE of 65–75 ms, TR of 2,500–3,700 ms, slice thickness of 4 mm with a 1 mm gap, matrix of 245×256, FOV 120 mm and NEX of 1. The 3 T protocol was the same as utilized for the cadaveric wrists, as described in the following.

All images were reviewed by a board certified, fellowship-trained musculoskeletal radiologist with 12 years of experience. Normal tendons typically show low or absent signal on both T1- and T2-weighted images, with increased signal typically seen in tendinosis or tear. The ECU was reviewed for low/normal or increased signal in all three planes, but for the purposes of this study, the axial images were selected for evaluation as the ECU pseudolesion is only seen in this plane.

Cadavers

A total of 10 cadaveric forearms (6 embalmed and 4 unembalmed) were harvested from 6 cadavers (4 embalmed and 2 unembalmed) at the Gross Anatomy Laboratory of our institution. The ages of the cadavers ranged from 65 to 87 years, four were females and two were males. None had a history of labor-intensive work. Four tendons (two right and two left) were harvested from fresh, frozen cadavers, and six were from embalmed cadavers (four right and two left). All arms were resected at the distal humeral diaphysis proximal to the origins of the ECU, to prevent any distortion that may occur with tendon retraction.

MRI

The cadaveric wrists were then scanned with a Siemens Verio 3.0 Tesla MRI. Axial spin echo T1 and fat suppressed fast spin echo T2-weighted images were acquired using a dedicated wrist coil, with the arm simulating the "superman" position. The T1-weighted imaging parameters were TE of 10–15 ms, TR of 500–800 ms, slice thickness of 4 mm with a 1.2 mm gap, matrix of 256×230, FOV of 120 mm and NEX of 3. T2-weighted parameters were TE of 65–75 ms, TR=2400-3500 ms, slice thickness of 4 mm with a 1.2 mm gap, matrix of 320×320, FOV of 120 mm and NEX of 1.

MicroCT

As the maximum object size permissible for the Skyscan 1172 scanner is 5 cm, the entire forearm could not be scanned; therefore, an approximately 4-cm segment of ECU tendon was removed after MRI, centered at the base of the ulna styloid process in the expected position of the pseudolesion. The tendons were tied to rigid plastic rods with silk suture material prior to being placed into fixative. The plastic rods prevented the tendons from twisting and buckling during the fixation process, which allowed for improved imaging with microCT. Four ECRB tendons from two embalmed cadavers were also resected for comparison.

The tendons were immersion fixed in 4 % paraformaldehyde in 0.1 M PO4 buffer, then immersion stained intact in 2 % phosphotungstic acid, 0.02 % potassium permanganate, and 0.1 % hematoxylin solution (phosphotungstic acid-hematoxylin or PTAH), before high resolution microCT scanning. The tendons were then scanned in a Skyscan 1172 microCT unit, using an isotropic voxel size of 12.8 μm, a source voltage of 100 kV, and a current of 100 μA. Three-dimensional (3D) reconstruction was performed using Skyscan N-recon software and measurements were made using Skyscan CTAn software.

The MR images were then directly compared to the microCT images. Regions of increased T1 and/or T2 signal were correlated with the microCT images based on their distance from the base of the ulna styloid process. The amount of hypo-attenuating inter or intra-tendinous material on microCT, and the orientation of the tendon fibers with respect

to the longitudinal axis was evaluated by the fellowship-trained musculoskeletal radiologist.

Histology

Tendon samples were then sectioned in order to obtain a histological specimen suitable for microscopy, in the regions of interest determined by MRI and microCT. Several samples were also taken from regions that demonstrated normal signal on MRI, for comparison. Samples were stained with Alcian blue and Safranin O to assess mucoid material, and Masson's trichrome stain to look for collagen, prior to light microscopy (magnification ×20). Evaluation and quantification of the mucoid material and collagen was performed by a cell biologist with 33 years of experience, and who is specialized in the effects of repetitive strain on biological tissues.

Results

Clinical cases

Of the 50 MRI studies, 64 % were male and 36 % were female patients, with ages ranging from 22 to 74 years and a mean age of 43 years—31 were right wrists, and 19 left. A total of 26 patients had associated radiographs, while none had associated fractures of the ulna styloid process, heterotopic ossification or post-surgical changes. Increased T1 signal alone was seen in 6 %, increased T2 signal alone was seen in 8 %, increased T1 and T2 signal was seen in 80 % (Fig. 1) and 6 % showed no perceptible increased signal in either pulse sequence. The increased signal was centrally located within the tendon in all cases, with a surrounding rim of tissue that was homogenously dark on both pulse sequences. The increased central signal intensity was subjectively graded into mild, moderate or severe by the board certified radiologist—75 % was classified as mild, 20 % as moderate and 5 % as severe. None of the cases had enlargement of the tendon, diffuse increased signal or associated tenosynovitis. Thirty-two cases were performed on the 1.5 Tesla MRI, and 18 on the 3 T scanner, with no significant difference in the prevalence and signal intensity between the two field strengths and the different patient positions, or whether left or right sided.

Cadavers

MRI

Twenty central regions of interest (ROI) at the base of the ulna styloid process were selected from the 10 tendons, two in each tendon. Two adjacent ROIs were selected for each tendon as the ulna styloid could not be used as a reference point after tendon resection, with the expected location of the pseudolesion determined by measurement. Nine out of the 10 ECU tendon samples (18 ROIs) showed varying degrees of central increased signal, and one tendon (2 ROIs) showed no increase. In six of these 18 ROIs (33.3 %), the increased signal was barely perceptible on both T1- and T2-weighted images. Twelve ROIs demonstrated definite and readily perceptible central increased signal (66.6 %; Fig. 2). Five of these 12 ROIs only demonstrated increased T1 signal (42 %) and 7 of the 12 ROIs demonstrated both increased T1 and T2 signal (58 %), whereas none of the tendons showed increased T2 signal alone. In all tendons, the periphery of the tendon showed homogenously low T1 and T2 signals. The age of the cadaver did not affect the prevalence and intensity of the increased signal; however, all cadavers were over 65 years of age. In no cadaver was an accessory extensor digiti minimi tendon present. MRI of the ECRB tendons showed no increased signal on T1- or T2-weighted images either centrally or peripherally (Fig. 1c), and no inter-tendinous ground substance was identified on microCT or histology (as described further in the following).

MicroCT

The fibers of the distal ECU underwent a gentle spiral along the longitudinal axis, with a maximum angulation of 8.39° at the level of the ulna styloid process (Figs. 3 and 8a). Analysis of the 12 ROIs (that showed significant increased signal on MRI) using microCT demonstrated a large amount of inter-tendinous curvilinear hypoattenuating material between the

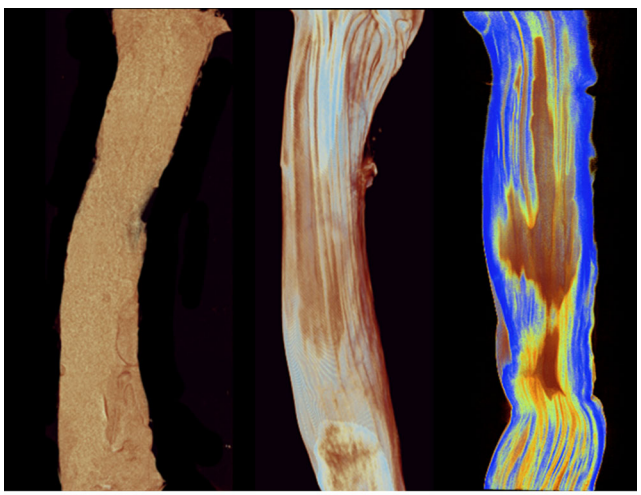

Fig. 3 71-year-old female cadaver. MicroCT. **a** Unstained tendon. Note that individual tendon fibers cannot be visualized. **b**–**c** Tendons were stained using phosphotungstic acid-hematoxylin (PTAH) which is composed of 2 % phosphotungstic acid, 0.02 % potassium permanganate, 0.1 % hematoxylin in dH2O. **c** 3D volume rendered image with color thresholding. Primary collagen fiber bundles are clearly visible in PTAH-stained tendons (compare **b** or **c** with **a**). All tendons were scanned in a Skyscan 1172 microCT scanner

two distal heads of the ECU tendons, corresponding to regions of increased central ground substance on histology and increased signal on MRI (Fig. 4). Furthermore, the six ROIs that showed barely perceptible central increased signal showed a smaller amount of inter-tendinous hypoattenuating material compared to the tendons that showed more significant increased signal.Control ECRB tendons showed scant intra-tendinous ground substance and no inter-tendinous ground substance, with the tendon fibers near parallel to the longitudinal axis.

Histology

Histologic evaluation of the 12 ROIs that demonstrated definite increased MRI signal showed an increased amount of stainable material using Alcian blue and Safranin O stains (indicating the presence of mucoid material), and Masson's trichrome stain (representing increased presence of collagen fibers; Figs. 5 and 6), with the intensity of the MR signal increasing with the amount of mucoid material. The histologic samples also showed that there was a smaller volume of stainable material within regions of the tendon that demonstrated barely perceptible or no increased T1 and/or T2 signal (either centrally or peripherally), indicating scant mucoid material and collagen.

None of the ECRB tendons showed increased T1 or T2 signal, and there was only a small amount of intra-tendinous ground substance or mucoid material on histology or microCT (Figs. 5b and 7a,b). Because the ECRB is only a single tendon and therefore cannot have inter-tendinous ground substance, the absence of central high signal is to be expected. Of interest, none of the ECRB fibers approached the magic angle on microCT, with the fibers nearly parallel to the longitudinal axis (Fig. 8b).

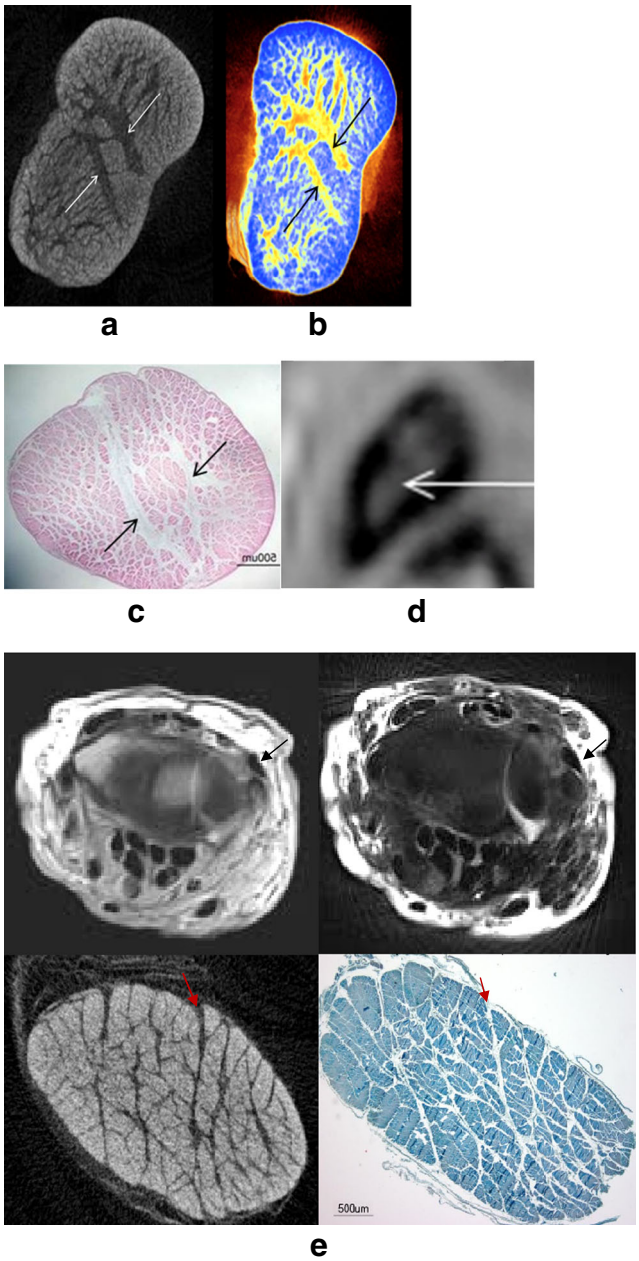

Fig. 4 71-year-old female cadaver. **a** Reconstructed axial microCT image through the region of increased MRI signal demonstrating linear regions of hypoattenuation (*white arrows*) between the two distal heads of the ECU tendon. **b** 3D volume rendered image using interactive transfer function to adjust colors and transparency to distinctly separate intra- and inter-tendinous ground substance (*yellow/orange*, indicated by *arrows*) from denser collagen tendon fibrils (*blue*). Note the relative paucity of ground substance within the peripheral tendon. **c** Safranin O stained slide (magnification ×20) shows the central inter-tendinous ground substance (*arrows*), corresponding to the hypoattenuating material seen centrally on microCT. **d** T1-weighted image at the same level shows central hyperintensity corresponding to the areas indicated in **a**, **b** and **c**. The paucity of peripheral ground substance results in peripheral low signal on MRI. **e** 65-year-old female cadaver with no increased signal for comparison. Axial T1- and T2-weighted images shows homogenous low signal intensity in the ECU tendon, without central increased signal (*black arrows*). Corresponding microCT and Alcian blue histology image shows a relative paucity of central inter-tendinous ground substance, making the separation of two distinct distal ECU heads (*red arrows*) difficult

Discussion

A tendon is composed of multiple strands of organized collagen fibers (predominantly type I collagen), elastin, and a proteoglycan-water matrix (ground substance). A group of collagen fibrils form a tendon fiber, the basic unit of a tendon (the smallest component visible with light microscopy). Tendon fibers are surrounded by a fine sheath of loose connective tissue called the endotenon. The endotenon binds a group of fibers to form a primary fiber bundle (subfasicle) and a group of primary fiber bundles makes a secondary fiber bundle. Likewise, a group of secondary bundles makes a tertiary bundle. The tertiary bundles makes up the tendon, which is surrounded by another connective tissue sheath called the epitenon [6]. There have been several reported reasons for increased T1 and/or T2 signal within tendons, some reflecting

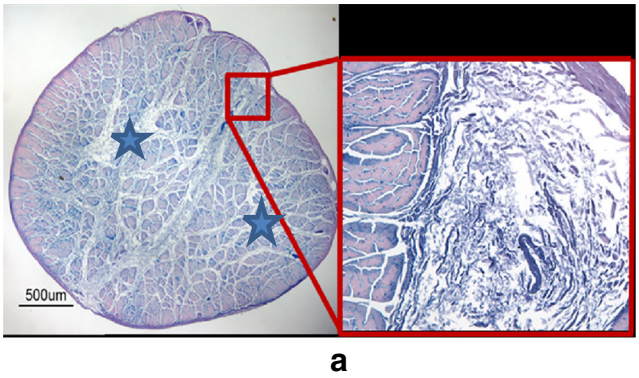

Fig. 5 76-year-old male cadaver. **a** Light microscopy (magnification ×20): Alcian blue staining corresponding to the regions of interest on MRI and microCT. Inter-tendinous (between the 2 distal heads of the ECU, represented by the *blue stars*) ground substance (*see inset*) corresponds with increased signal intensity on axial MRI and hypo-attenuated areas on PTAH-stained axial microCT scans. Alcian blue detects the presence of mucoid material by staining acid mucosubstances and acetic mucins (*stained blue*). **b** Quantification of the percent area stained with Alcian blue clearly demonstrates a significant increase in the ECU compared to control extensor carpi radialis brevis (ECRB) tendons, with those ECU tendons with higher quantification demonstrating more intense signal on MRI

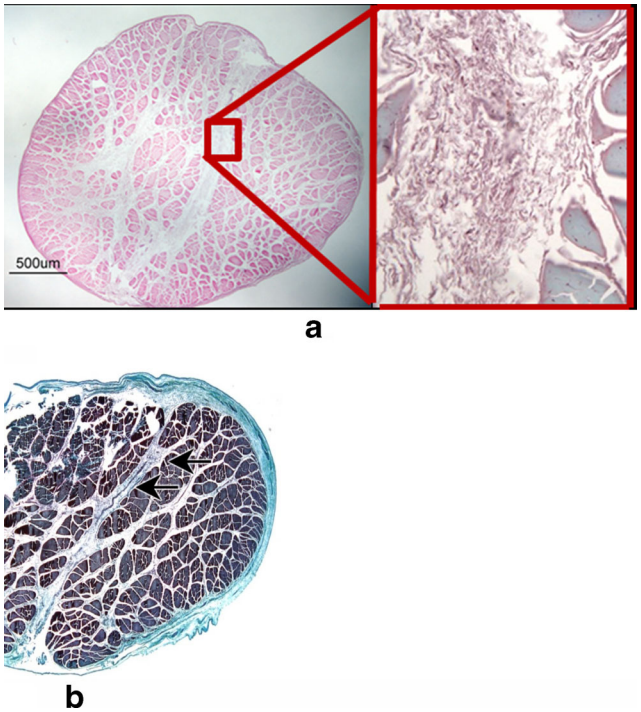

Fig. 6 76-year-old male cadaver. Light microscopy (magnification ×20). **a** ECU tendon stained with Safranin O (stained proteoglycans pink) demonstrating mucoid material in the inter-tendinous ground substance (see *inset*). **b** Masson's trichrome demonstrating regions of high collagen deposition within the loose connective tissue that constitutes the inter-tendinous ground substance (*black arrows*), indicating tendon degeneration

a true pathologic process, others reflecting normal variations or artifact.

The magic angle phenomenon is an MRI artifact resulting in increased intra-tendinous signal on short TE sequences (T1, proton density, and gradient echo images). The artifact usually occurs in tissues with well-ordered collagen, such as tendons, ligaments and cartilage, and the signal disappears on longer TE sequences. This is a well-documented phenomenon that occurs when a tendon lies close to the "magic angle" of 54.74° to B0 (commonly referenced as 55°) [7, 8], and the effect appears to be somewhat reduced at 3 Tesla [9]. At the magic angle, there is loss of the dipole interaction between two spinning nuclei which normally leads to reduced signal intensity, and the T2 decay is then decelerated, resulting in increased signal. This artifact can occur in any tendon that lies close to the magic angle in the standard scanning position and is commonly seen in the extensor pollicis longus tendon, the peroneus longus and brevis tendons of the ankle, the supraspinatus tendon, and the long head of biceps tendons. It can also be seen in ligaments such as the posterior cruciate ligament, and in the collateral ligaments of the ankle, for example the posterior talofibular ligament [7]. The scapholunate and lunotriquetral ligaments of the wrist may also be affected, as well as the ulna nerve as it passes into Guyon's canal [10, 11]. Other causes of increased T1 signal in tendons are well known and are caused by proteinaceous fluid, fat, or mucoid material within the tendon. The most common causes of T1 shortening are mucoid degeneration, fatty infiltration at the entheses, and fat containing accessory ossicles [12, 13]. Increased T2 signal may be caused by tendinosis, tear or the presence of a fibrocartilaginous node [14]. Tendinosis or tear can be differentiated from the ECU pseudolesion by the presence of tendon enlargement or attrition, and diffuse (not central) increased signal intensity [4]. A fibrocartilaginous node would be expected to be hyperintense on fat suppressed T2-weighted images, and low signal on the T1-weighted images [14]. In addition, lipoid or fatty infiltration of the tendons may show fat suppression on fat suppressed T2-weighted images, unlike the ECU pseudolesion.

The ECU muscle is composed of two bellies, one originating from the lateral epicondyle of the humerus and the other from the posterior border of the ulna, with the two distal heads (of these separate origins) inserting on the base of the fifth metacarpal [5, 15, 16]. The extensor carpi radialis brevis

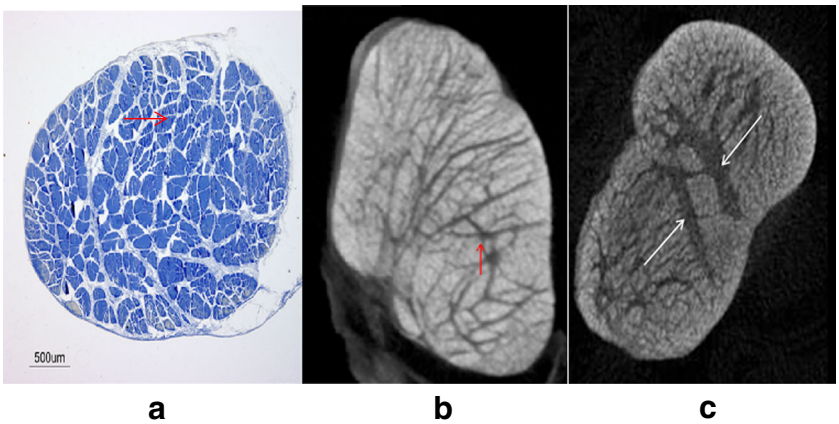

Fig. 7 71-year-old female cadaver. ECRB tendon. Alcian blue staining on light microscopy (magnification ×20) shows a smaller amount of intra-tendinous ground substance and mucoid material (*red arrow*), and there is no inter-tendinous ground substance (the ECRB has only one origin and one distal head). **b** Corresponding microCT image shows a small amount of intra-tendinous ground substance (*red arrow*), and no inter-tendinous ground substance. The amount of intra-tendinous ground substance in the ECRB is not of sufficient volume to produce a detectable signal on MRI. **c** ECU for comparison shows the increased inter-tendinous ground substance (*white arrows*) responsible for increased central signal on MRI. Note the peripheral intra-tendinous ground substance is similar to the ECRB, accounting for the peripheral low signal seen in all ECU tendons

tendon, on the other hand, has a single origin from the lateral epicondyle of the humerus, and a single distal head inserting at the base of the third metacarpal (15). Kalson et al. demonstrated that the two distal tendons of the ECU spiral at 8° to the longitudinal axis at the level of the ulna styloid process, the region of typical increased signal, which would not cause a significant change in angulation in relation to B0 to produce a magic angle artifact [5]. This is supported by our findings with the tendon fibers spiraling at a maximum of 8.39° to the longitudinal axis, discounting magic angle effect as the etiology. In addition, the T2 signal would be expected to be normal as the magic angle effect disappears on longer TE sequences. Peh et al. have quoted a critical threshold TE of 37 ms on conventional spin echo (CSE) imaging [17], above which the artifactual signal vanishes. Li et al. have also reported that the critical TE varies according to the pulse sequence [18]; however, this is not the case with the ECU pseudolesion, as in the majority of cases the signal on T2-weighted images (with long TEs) is also high. Our histology samples showed that every one of the six tendons (12 ROIs) with significantly increased central MRI signal demonstrated an increased amount of ground substance, collagen and mucoid material between the two distal tendon heads (Figs. 5 and 6), consistent with chronic degenerative changes [19], and the increased inter-tendinous MRI signal likely represents T1 shortening and T2 prolongation from the mucoid material. It is unclear why five of these ROIs demonstrated T1 hyperintensity alone, as mucoid material should also result in T2 hyperintensity. The isolated T1 hyperintensity occurred in both embalmed and unembalmed specimens, but we theorize that this may be related to tissue atrophy and dehydration that occurs in the post mortem state [20, 21], and the cross linkage of proteins that occurs in embalmed cadavers [22]. Similarly, no tendon demonstrated increased T2 signal alone, again presumably due to tissue dehydration. The three tendons (six ROIs) with barely perceptible increased central T1 and T2 signal had a smaller amount of inter-tendinous ground substance with only minimal mucoid and collagen.

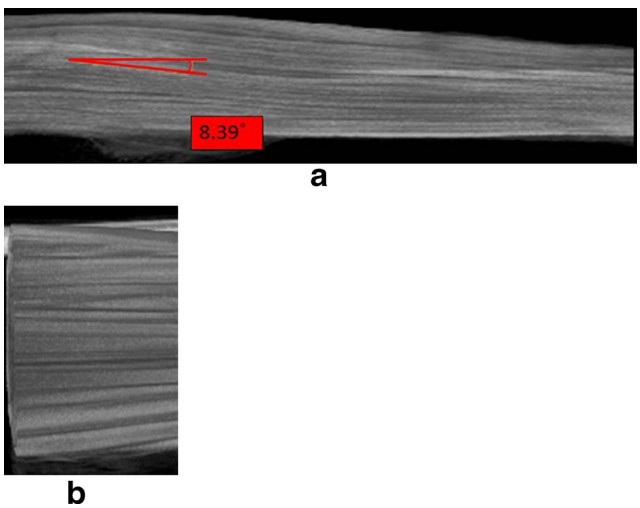

Fig. 8 71-year-old female cadaver. **a** MicroCT shows gentle spiraling of the distal ECU tendon fibers, and the fibers are at a maximum of 8.39° to the longitudinal axis of the tendon. **b** MicroCT of a comparison ECRB tendon shows the fibers are near parallel to the longitudinal axis

Our analysis of the ECU tendon demonstrates a strong association between central increased signal (either T1 alone, or increased T1/T2) and an increased volume of central inter-tendinous ground substance seen on microCT. The central inter-tendinous ground substance on microCT was volumetrically much more than the peripheral intra-tendinous ground substance in all tendons, accounting for the lack of signal in the peripheral tendon, and these findings were supported by

histology which demonstrated an increased amount of central intra-tendinous ground substance as well as mucoid and collagen material.

Furthermore, all cadaveric ECU tendons that demonstrated barely perceptible increased central MRI signal showed a smaller amount of central inter-tendinous ground substance and collagen on microCT, with minimal mucoid material on histologic evaluation. These findings suggest that although the presence of normal ground substance between the two distal heads of the ECU may result in central increased signal in normal tendons, a critical volume threshold is needed before the signal is perceptible. The intensity of the signal in the tendon is related to the amount of mucoid and collagen material, which are typically increased in tendon degeneration. This is supported by the findings in the control ECRB tendons, where scant intra-tendinous ground substance and mucoid material, and no inter-tendinous ground substance, resulted in no perceptible signal on MRI. It is reasonable to assume that with increasing severity of tendon degeneration, the peripheral intra-tendinous ground substance and stainable material (in any tendon) may reach a critical threshold where the entire tendon shows increased signal on MRI.

Limitations to this study include non-blinded data and results for the radiologist and anatomist, which limits intra-observer variability. There were also no surgical reports or surgical/anatomic correlation of the ECU pseudolesion in the retrospectively reviewed clinical MRIs. The cadaver wrist positioning in the MRI scanner may not have been the same as the clinical cases (due to rigidity of the post mortem state) and this may alter the signal characteristics. Finally, some distortion may occur in the microCT specimens after resection and anchoring to a plastic rod.

Conclusion

Ulnar-sided wrist pain is a common entity with a wide differential diagnosis. Central increased T1 and/or T2 signal in the ECU is frequently seen, and is often misinterpreted as tendinosis or "magic angle" artifact. MicroCT however shows that the tendon fibers never approach the "magic angle", discounting this artifact as the etiology. MicroCT and histology show that the signal is a result of the normal inter-tendinous ground substance located centrally between the two distal heads of the ECU at the level of the ulna styloid process. A critical volume of ground substance is needed before the signal is perceptible, with increased mucoid and collagen material (as seen in tendon degeneration) resulting in an increased intensity of the signal. It is unclear whether there is any correlation between the findings of mucoid degeneration and patient symptomatology. Further investigation correlating the clinical picture (utilizing a standardized tool) with qualitative and quantitative MRI parameters may be justified.

Acknowledgments Roshanak Razmpour, for preparation of the histology slides.

Author disclosure Nothing to disclose

Conflict of interest There are no conflicts of interest

References

1. Porteous R, Harish S, Parasu N. Imaging of ulnar-sided wrist pain. Can Assoc Radiol J. 2012;63(1):18–29. doi:10.1016/j.carj.2010.07.007.
2. Lichtman DM, Alexander AH, editors. The wrist and its disorders. 2nd ed. Philadelphia, Pa: Saunders; 1997.
3. Taleisnik J. Pain on the ulnar side of the wrist. Hand Clin. 1987;3(1):51–68.
4. Timins ME, O'Connell SE, Erickson SJ, Oneson SR. MR imaging of the wrist: normal finding that may simulate disease. Radiographics. 1996;16:987–9955.
5. Kalson NS, Malone PSC, Bradley RS, Withers PJ, Lees VC. Fibre bundles in the human extensor carpi ulnaris tendons are arranged in a spiral. J Hand Surg Eur Vol. 2012;37:550–4.
6. Kannus P. Structure of the tendon connective tissue. Scand J Med Sci Sports. 2000;10:312–3207.
7. Erickson SJ, Cox IH, Hyde JS, Carrera GF, Strandt JA, Estkowski LD. Effect of tendon orientation on MR imaging signal intensity: a manifestation of the "magic angle" phenomenon. Radiology. 1991;181(2):389–928.
8. Erickson SJ, Prost RW, Timins ME. The "magic angle" effect: background physics and clinical relevance. Radiology. 1993;188(1):23–5.9.
9. Gold GE, Suh B, Sawyer-Glover A, Beaulieu C. Musculoskeletal MRI at 3.0 T: initial clinical experience. AJR Am J Roentgenol. 2004;183(5):1479–86.10.
10. Burns JE, Tanaka T, Ueno T, Nakamura T, Yoshioka H. Pitfalls that may mimic injuries of the triangular fibrocartilage and proximal intrinsic wrist ligaments at MR imaging. Radiographics. 2011;31(1):63–78.
11. Chappell KE, Robson MD, Stonebridge-Foster A, et al. Magic angle effects in MR neurography. AJNR Am J Neuroradiol. 2004;25(3):431–40.
12. Buck FM, Grehn H, Hilbe M, Pfirrmann CWA, Manzenell S, Hodler J. Degeneration of the long biceps tendon: comparison of MRI with gross anatomy and histology. Am J Roentgenol. 2009;193:1367–75.
13. Rosenberg ZS, Beltran J, Bencardino JT. From the RSNA refresher courses. Radiological Society of North America. MR imaging of the ankle and foot. Radiographics. 2000;20:S153–79.
14. Didolkar MM, Malone AL, Nunley II JA, Dodd LG, Helms CA. Pseudotear of the peroneus longus tendon on MRI, secondary to a fibrocartilaginous node. Skelet Radiol. 2012;41:1419–25.
15. Moore K, Agar A. Essential clinical anatomy. 2nd ed. Lippincott; 2002.
16. Tountas CP, Bergman RA. Anatomic variations of the upper extremity. New York: Churchill Livingstone; 1993. p. 126–8.
17. Peh WCG, Chan JHM. The magic angle phenomenon in tendons: effect of varying the MR echo time. Br J Radiol. 1998;71:31–6.
18. Li T, Mirowitz SA. Manifestation of magic angle phenomenon: comparative study on effects of varying echo time and tendon orientation among various MR sequences. Magn Reson Imaging. 2003;21:741–4.

19. Khan KM, Cook JL, Bonar F, Harcourt P, Astrom M. Histopathology of common tendinopathies update and implications for clinical management. Sports Med. 1999;6:393–408.
20. Terrall KR, Harper ML, Rispin KL, Ayers S, Gonzalez RV. Procuring relevant soft tissue data for use in computational modeling. 25th Annual Houston Conference on Biomedical Engineering Research. Houston; 2008.
21. Viidik A, Lewin T. Changes in tensile strength characteristics and histology of rabbit ligaments induced by different modes for postmortal storage. Acta Orthop Scand. 1996;37:141–55.
22. Huang D, Chang TR, Aggarwal A, Lee RC, Ehrlich HP. Mechanism and dynamics of mechanical strengthening in ligament-equivalent fibroblast-populated collagen. Ann Biomed Eng. 1993;21(3):289–305.